Detection and counting of bean plants using UAV-acquired RGB imagery and YOLOv8 models

Girley F. Valdes[1]*, Thiago O. C. Barboza[1], Raí Q. Alves[1],

Matheus Arnosti[1], Gustavo L. Silveira[1], Octavio Pereira[1],

Wender H. Batista da Silva[1], Adão F. dos Santos[1]

[1] Federal University of Lavras (UFLA), Lavras, MG, Brazil

*Corresponding author: girley.fernandez1@estudante.ufla.br

A paper from the Proceedings of the
17th International Conference on Precision Agriculture and 11th Brazilian Congress on Precision and Digital Agriculture
13-15 July 2026
Porto Alegre, Brazil

Abstract

Accurate plant stand assessment during early crop development is essential for evaluating crop establishment and supporting management decisions in common bean production. However, manual plant counting is labor-intensive, time-consuming, and limited in its ability to represent spatial variability across the field. This study evaluated the performance of five YOLOv8 object detection models (Nano, Small, Medium, Large, and Extra Large) for identifying and counting common bean (Phaseolus vulgaris L.) plants using high-resolution RGB images acquired by an unmanned aerial vehicle (UAV) at different flight heights. The experiment was conducted in a common bean field planted with cultivar IAC 2051 at the Federal University of Lavras, Brazil. RGB images were acquired using a DJI Mavic 3M UAV at two flight heights, 20 and 40 m above the crop canopy. The images were processed into orthomosaics, cropped into 640 × 640 pixel patches, annotated, and used to train, validate, and test five YOLOv8 architectures: Nano, Small, Medium, Large, and Extra Large. Model performance was evaluated using precision, recall, mAP50, mAP50–95, and classification loss curves. Automatic plant counting was validated against manual field counts obtained from 25 sampling points using R^2, RMSE, and MAE. Flight height directly affected model performance. Images acquired at 20 m provided better overall detection results, indicating that higher spatial resolution favored the identification of small plants at the V2 stage. Under these conditions, lightweight models showed competitive performance, with YOLOv8s achieving the highest mAP50 value (0.749) and YOLOv8n showing the highest recall (0.758). At 40 m, detection performance decreased; however, YOLOv8l showed the best

The authors are solely responsible for the content of this paper, which is not a refereed publication. Citation of this work should state that it is from the Proceedings of the 17th International Conference on Precision Agriculture and 11th Brazilian Congress on Precision and Digital Agriculture. EXAMPLE: Last Name, A. B. & Coauthor, C. D. (2026). Title of paper. In Proceedings of the 17th International Conference on Precision Agriculture and 11th Brazilian Congress on Precision and Digital Agriculture (unpaginated, online). Monticello, IL: International Society of Precision Agriculture and Brazilian Congress on Precision and Digital Agriculture.

performance among the evaluated architectures, with mAP50, mAP50–95, and precision values of 0.569, 0.231, and 0.709, respectively. For plant counting, YOLOv8m showed the highest R^2 at 20 m (0.436), whereas YOLOv8l achieved the best counting performance at 40 m, with $R^2 = 0.394$, RMSE = 5.064, and MAE = 4. 280.These findings demonstrate that UAV-acquired RGB images and YOLOv8 models have potential for automatic common bean plant detection and counting during early crop development. The results also indicate that flight height and model architecture should be selected according to the monitoring objective, balancing spatial resolution, field coverage, and counting accuracy.

Keywords. *Deep learning, UAV, computer vision, artificial intelligence, plant counting, YOLOv8.*

Introduction

Common bean (*Phaseolus vulgaris* L.) has high economic and social importance in Brazil, being one of the main crops used to supply food to the population (FAO, 2023; Oliveira & Wander, 2023). Brazil is among the largest producers and consumers of common bean worldwide, highlighting the importance of strategies that contribute to increasing the productive efficiency of this crop (CONAB, 2026; FAO, 2023).

Given the importance of common bean in Brazilian agriculture, achieving the recommended plant population during sowing is essential, as plant population is one of the main factors determining the productive potential of the crop (Donato et al., 2022). Emergence failures, sowing problems, adverse soil conditions, and pest and disease incidence can significantly reduce the number of plants established in the field (Biezus et al., 2017; Quintela & Barbosa, 2015; Silva & Heinemann, 2023). Therefore, the identification and counting of the initial plant stand are fundamental for assessing crop establishment quality and supporting agronomic decision-making.

Validation of plant population is particularly important during the early growth stages of the crop, when corrective interventions, such as reseeding, can still be performed in areas with establishment failures. However, conventional plant counting methods are generally performed manually, requiring considerable time and labor, especially in large areas (Kitano et al., 2019). In addition, assessments based on only a few sampling points may not adequately represent the spatial variability present in the cultivated area.

In this context, digital agriculture and precision agriculture have incorporated new technologies to automate crop monitoring. Among these technologies, unmanned aerial vehicles (UAVs) stand out due to their ability to acquire high-spatial-resolution images in a short period of time, enabling rapid and non-destructive monitoring of agricultural areas (Radoglou-Grammatikis et al., 2020; Tsouros et al., 2019). Similarly, advances in artificial intelligence and deep learning have expanded the possibilities for automatically extracting relevant information for crop management from images (Chen et al., 2023; Zhu et al., 2024). Single-stage object detection models, such as those belonging to the YOLO (You Only Look Once) family, have gained attention due to their high processing speed and accuracy in object identification. These models simultaneously perform object localization and classification, making them especially suitable for real-time applications (Alif & Hussain, 2024). The YOLO family has been widely used in different agricultural applications, including plant identification, disease detection, crop monitoring, and yield estimation (Rana & Vaidya, 2026).

Among the different architectures available, YOLOv8 stands out as a version that presents improvements in feature extraction and object detection at different scales, making it a promising alternative for agricultural applications based on UAV-acquired imagery (Barboza, Fernandez, et al., 2026; Sapkota et al., 2025).

Despite these advances, the application of object detection models in agricultural environments still presents important challenges. The spatial variability of cultivated areas, associated with differences in soil background, vegetation cover, and lighting conditions, can directly influence model performance (Barboza, Santos, et al., 2026). In addition, although UAVs enable rapid monitoring of large agricultural areas, limited information is still available on the influence of flight height on the automatic identification and counting of common bean plants during early growth stages. Since flight height directly affects the spatial resolution of images, different altitudes may alter the ability of models to correctly detect plants in the field (Barboza, Santos, et al., 2026; Lu et al., 2023). Therefore, understanding the effect of flight height is essential to optimize image acquisition and increase the accuracy of automatic detection systems under real cropping conditions.

Thus, the objective of this study was to evaluate the influence of different flight heights on the performance of YOLOv8 models for the identification and counting of common bean plants using UAV-acquired RGB imagery.

Materials and Methods

Study location and characterization

The study was conducted at the Center for Development and Technology Transfer (CDTT) of the Federal University of Lavras (UFLA), located in Ijaci, Minas Gerais, Brazil (21°09′ S, 44°54′ W). The regional climate is classified as Cwa according to Köppen, characterized by a dry winter and a rainy summer. The experimental area had clayey soil, and soil fertility management was performed according to recommendations based on soil chemical analysis.

Common bean (*Phaseolus vulgaris* L.), cultivar IAC 2051, belonging to the Carioca commercial group, was cultivated under a no-tillage system during the 2025 growing season. The cultivar has an indeterminate type II growth habit, semi-erect architecture, and an average cycle of approximately 85 days. The crop was established in an area of approximately 5,000 m^2 (0.5 ha), using a four-row seed drill-fertilizer, with 0.60 m spacing between rows. The sowing density was adjusted to 17 seeds m^{-1}, resulting in an estimated final population of approximately 240,000 plants ha^{-1}. Phytosanitary and nutritional management were performed according to the technical recommendations for common bean cultivation.

UAV image acquisition and dataset preparation

RGB images were acquired on November 17, 2025, during the V2 phenological stage of common bean, using a DJI Mavic 3M unmanned aerial vehicle (UAV) (SZ DJI Technology Co., Shenzhen, China). Flights were conducted in automatic mode at two different flight heights, 20 and 40 m above the crop canopy (Figure 2).

(**A**) (**B**)

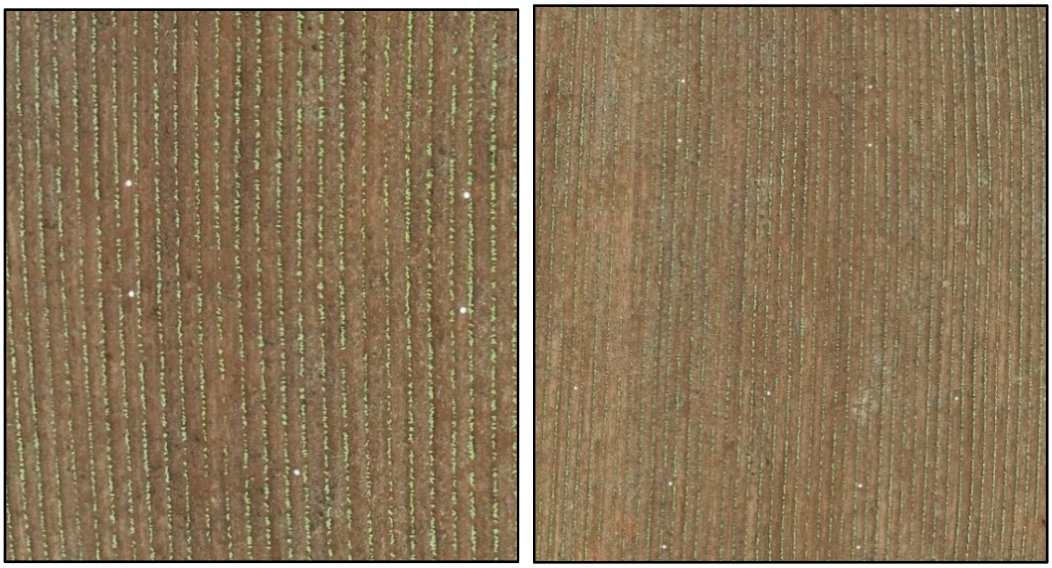

Figure 2. Field images acquired by UAV at flight heights of 20 m (A) and 40 m (B) during the V2 growth stage of common bean (*Phaseolus vulgaris* L.).

Images were acquired between 10:00 and 11:00 a.m. under partly clear sky conditions to reduce interference caused by shadows, wind, and lighting variations. Subsequently, the collected images were processed using Pix4D software to generate orthomosaics, which were exported in JPEG format. The orthomosaics were then cropped into 640 × 640 pixel images using a code developed in Python in Visual Studio Code.

After cropping, the images were labeled on the Roboflow platform using a single class named “F”, corresponding to common bean plants (Figure 3). During the export step, data augmentation techniques were applied, generating three versions of each image in the training set. The dataset was divided into 70% for training, 20% for validation, and 10% for testing. Data augmentation techniques were applied exclusively to the training set. The distribution of images used for training, validation, and testing at each flight height is presented in Table 1. The transformations applied included horizontal flipping, rotation between -15° and +15°, brightness variation between -15% and +15%, and exposure variation between -10% and +10%.

(**A**) (**B**)

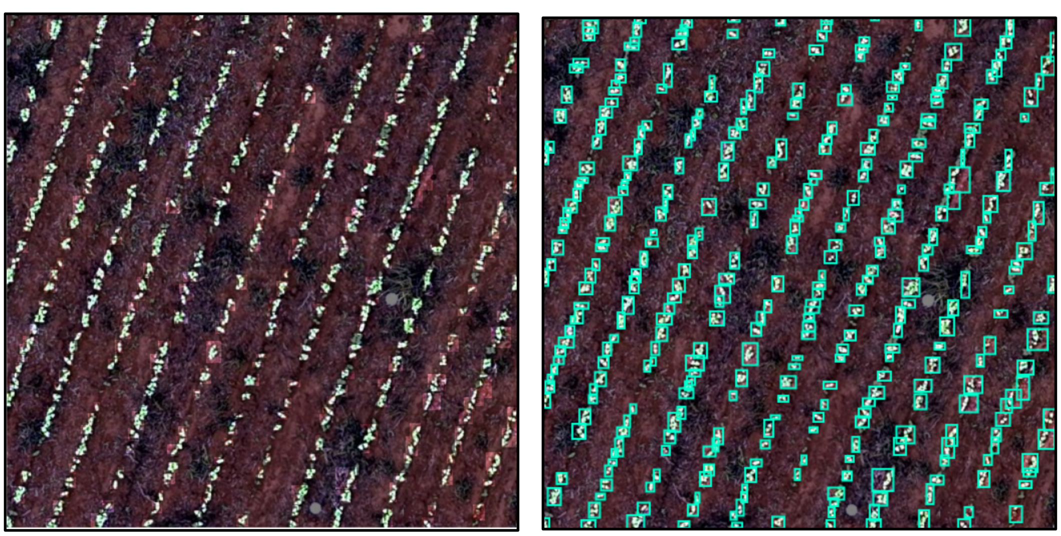

Figure 3. RGB image acquired by UAV and cropped to 640 × 640 pixels (A), and the corresponding labeling of common bean plants in the Roboflow platform (B).

Table 1. Dataset distribution for YOLOv8 training, validation, and testing at 20 and 40 m flight altitudes.

Flight altitude	Original images	Training images	Validation images	Test images	Total images
20 m	758	1,593	152	75	1820
40 m	176	368	35	18	421

The dataset was subsequently used for training and validating five YOLOv8 models: YOLOv8n (Nano), YOLOv8s (Small), YOLOv8m (Medium), YOLOv8l (Large), and YOLOv8x (Extra Large), using scripts developed in Python in Visual Studio Code. The process was divided into two stages: first, common bean plants were identified using the detection models; subsequently, the detected plants were counted.

To validate plant counting in the initial stand, 25 reference sampling points were established throughout the cultivated area. At each sampling point, white plates were positioned as reference markers in the central region of the evaluated area. Manual plant counting was performed along 3 linear meters of crop row at each sampling point, allowing comparison between the values observed in the field and those estimated by the YOLOv8 models.

The YOLOv8 models were trained using pretrained weights through transfer learning, with a maximum limit of 500 epochs. However, an early stopping parameter with a patience of 100 epochs was applied, automatically stopping training when no improvements in loss values were observed. The input images used for training had dimensions of 640 × 640 pixels. Images were loaded using eight workers, allowing parallel data processing according to the available computational capacity. Training was performed on an NVIDIA GeForce RTX 5070 Ti GPU with 16 GB of VRAM, using the SGD (Stochastic Gradient Descent) optimizer.

Performance metrics evaluation

The performance of the YOLOv8 models was evaluated using recall (Equation 1), precision (Equation 2), mean average precision at an Intersection over Union threshold of 50% (mAP50; Equation 3), and mean average precision considering IoU thresholds ranging from 50% to 95% (mAP50–95; Equation 4). These metrics were used to compare the ability of the models to correctly detect common bean plants in the images.

$$Recall = TPTP + FN \tag{1}$$

Recall (R) represents the proportion of objects correctly detected by the model. It is calculated based on true positives (TP) and false negatives (FN) and indicates the model's ability to detect common bean plants present in the images. High recall values indicate that most common bean plants were correctly identified, whereas low values suggest a higher occurrence of objects not detected by the model.

$$Precision = TPTP + FP \tag{2}$$

Precision (P) represents the proportion of correct detections made by the model in relation to the total number of detections performed. True positives (TP) represent correct detections, whereas false positives (FP) correspond to incorrect detections made by the model.

$$mAP50 = 1N \sum Ni = \mathrm{lAPyo} \quad (3)$$

mAP50 represents the mean average precision calculated considering an Intersection over Union (IoU) threshold of 50%. N refers to the number of samples evaluated, and AP represents the average precision values obtained by the model.

$$mAP50 - 95 = 1N \sum Ni = \mathrm{lAPyo} \quad (4)$$

mAP50–95 represents the mean average precision calculated at different Intersection over Union (IoU) thresholds, ranging from 50% to 95%. N refers to the number of samples evaluated, and AP represents the average precision values obtained by the model.

In addition to the detection metrics, the models were evaluated using the Train Cls Loss and Val Cls Loss curves. These metrics allowed the analysis of model behavior during training and the evaluation of learning evolution over the epochs. After training and validation, the models were used to identify and count common bean plants in the evaluated images.

Validation of plant counting

During the validation step, the number of common bean plants present at each sampling point in each image was initially determined by manual counting and subsequently compared with the values estimated by the YOLOv8 models. Additionally, linear regression analysis was performed to compare the observed values (manual counting) and predicted values (automatic counting), calculating the coefficient of determination (R^2; Equation 5), root mean square error (RMSE; Equation 6), and mean absolute error (MAE; Equation 7).

$$R^2 = 1 - \frac{\sum_{i=1}^{n}(y_i - \hat{y}_i)^2}{\sum_{i=1}^{n}(y_i - \bar{y}_i)^2} \quad (5)$$

$$RMSE = \sqrt{\frac{1}{n}\sum_{i=1}^{n}(} y_i - \hat{y}_i)^2 \quad (6)$$

$$MAE = \frac{1}{n}\sum_{i=1}^{n}|y_i - \hat{y}_i| \quad (7)$$

Results and Discussion

The performance of the YOLOv8 models varied according to flight height and model architecture. Models trained with images acquired at 20 m showed better detection results than those trained with images acquired at 40 m (Figures 5 and 6).

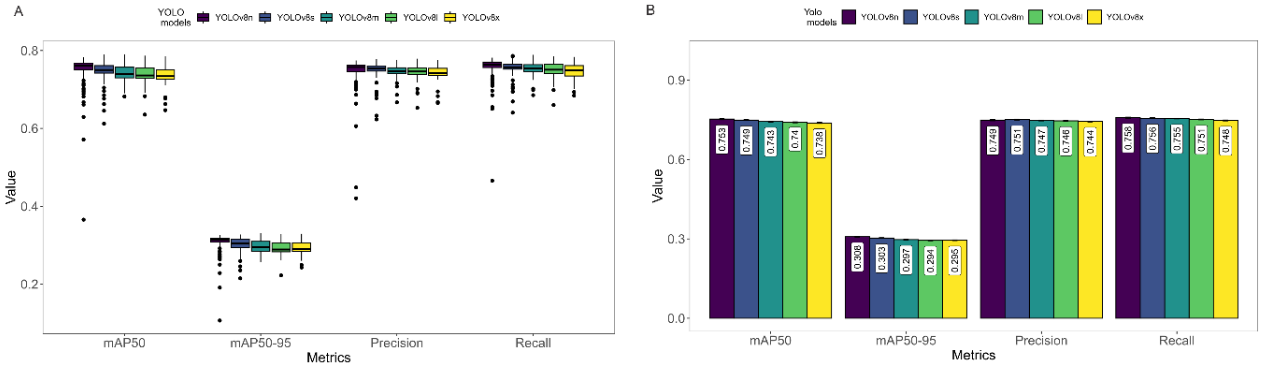

Figure 5. Performance metrics obtained by the YOLOv8 models for detecting common bean plants at the V2 phenological stage using UAV-acquired images at a flight height of 20 m. (A) Distribution of mAP50, mAP50–95, precision, and recall values represented by boxplots. (B) Mean values of the performance metrics evaluated for each YOLOv8 architecture.

For the flight height of 20 m, the results presented in Figure 5A indicate that the highest values were observed for mAP50, precision, and recall, demonstrating the ability of the models to identify common bean plants. In contrast, mAP50–95 showed lower values, indicating greater difficulty in the precise localization of bounding boxes. Regarding the distribution of the metrics, the YOLOv8n and YOLOv8s models showed greater stability and lower variability compared with the other architectures.

When comparing the mean values of the performance metrics (Figure 5B), the YOLOv8n and YOLOv8s models showed slightly superior performance. YOLOv8s obtained the highest mAP50 value (0.749), whereas YOLOv8n showed the highest recall (0.758). For precision, YOLOv8s and YOLOv8m presented similar values, with 0.750 and 0.747, respectively. For mAP50–95, the values were lower for all models, ranging approximately from 0.296 to 0.303. These results indicate that, at this flight height, lighter architectures were sufficient to identify common bean plants. In contrast, more complex models, such as YOLOv8l and YOLOv8x, did not achieve the highest mean performance values, suggesting that lighter architectures were adequate for plant identification and counting in images acquired at 20 m.

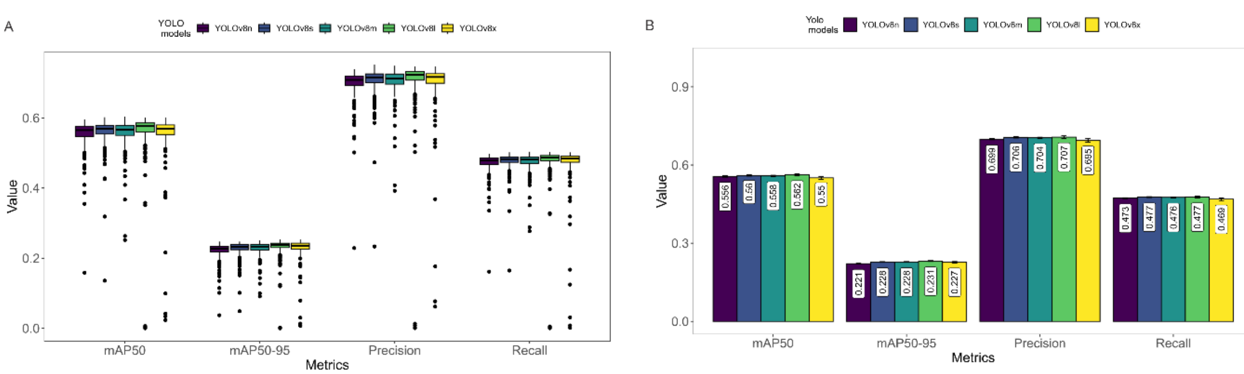

Figure 6. Performance metrics obtained by the YOLOv8 models for detecting common bean plants at the V2 phenological stage using UAV-acquired images at a flight height of 40 m. (A) Distribution of mAP50, mAP50–95, precision, and recall values represented by boxplots. (B) Mean values of the performance metrics evaluated for each YOLOv8 architecture.

For the flight height of 40 m, the results presented in Figure 6A show greater data dispersion and the presence of outliers, indicating higher variability in model performance. This behavior may be associated with the reduction in image spatial resolution caused by the increase in flight height, which makes it more difficult to identify small plants and plants located close to each other. The YOLOv8l model showed more stable behavior and better overall performance compared with the other architectures.

Compared with the results obtained at 20 m, a general reduction in the performance metrics was observed for the models evaluated at 40 m (Figure 6B), indicating greater detection difficulty with increasing flight height. While the YOLOv8n and YOLOv8s models showed the best performance at 20 m, the YOLOv8l model stood out at 40 m for mAP50, mAP50–95, and precision, with values of 0.569, 0.231, and 0.709, respectively. These results suggest that, in images acquired at greater flight heights, more complex models may have an advantage due to their greater capacity for feature extraction in images with a lower level of spatial detail.

In addition, the association between flight height and plant growth stage may alter the performance of YOLO models, since lower flight heights allow effective detection even with lightweight models, whereas higher altitudes, such as 70 m, may reduce detection capacity at the V2 and V6 stages, indicating the need for more advanced models under these conditions (Barboza, Santos, et al., 2026). Additionally, environmental factors, such as changes in leaf morphology, wind action, and lighting fluctuations, may cause plant occlusion, impairing the accuracy of the automatic detection process (Furlanetto et al., 2025).

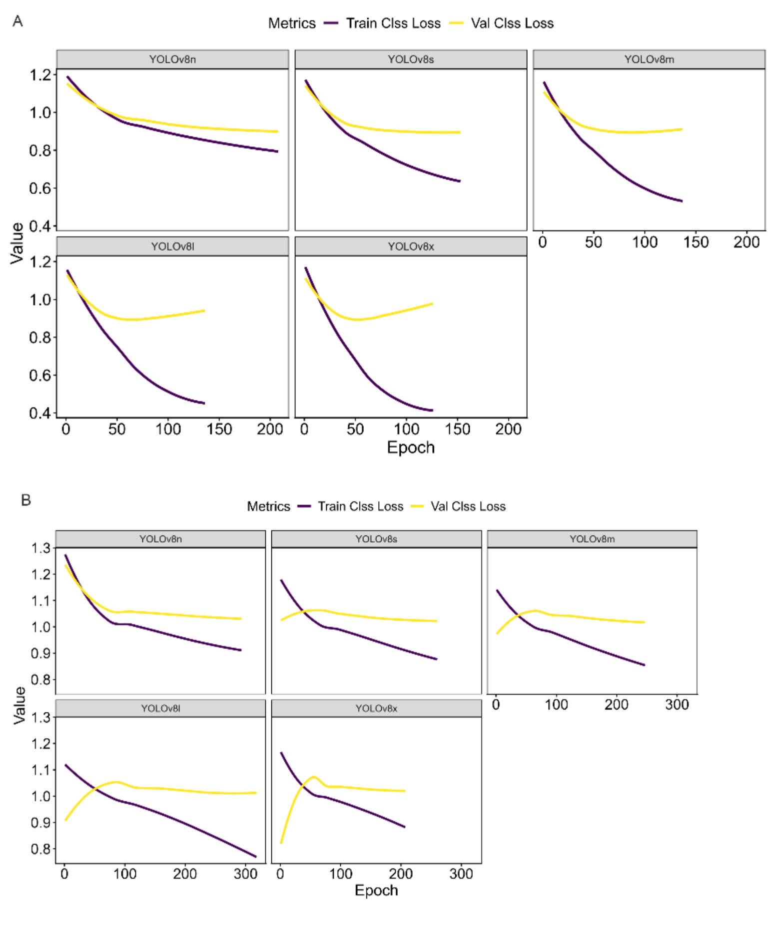

Figure 7. Training loss (Train Cls Loss) and validation loss (Val Cls Loss) curves for the YOLOv8n, YOLOv8s, YOLOv8m, YOLOv8l, and YOLOv8x models used for detecting common bean plants at the V2 phenological stage. Panels (A) and (B) correspond to flight heights of 20 and 40 m, respectively.

The training and validation loss curves indicated that all YOLOv8 models showed learning throughout the epochs (Figure 7). In general, training loss decreased progressively, demonstrating that the models were able to adjust their parameters to the data used during training. This behavior indicates a reduction in classification error as the number of epochs increased.

For the flight height of 20 m (Figure 7A), the lower-complexity models, such as YOLOv8n and YOLOv8s, showed a more gradual reduction in loss, indicating slower convergence during training. In contrast, models with a larger number of parameters, such as YOLOv8l and YOLOv8x, showed a faster reduction in training loss. In some cases, validation loss did not follow the same decreasing trend observed during training, suggesting lower generalization capacity and possible overfitting.

For the flight height of 40 m (Figure 7B), training loss also decreased throughout the epochs, indicating model learning. However, validation loss showed greater instability and tended to stabilize at higher values than training loss. This behavior suggests that, although the models learned the patterns present in the training dataset, the lower spatial resolution of the images acquired at 40 m may have made generalization to the validation dataset more difficult.

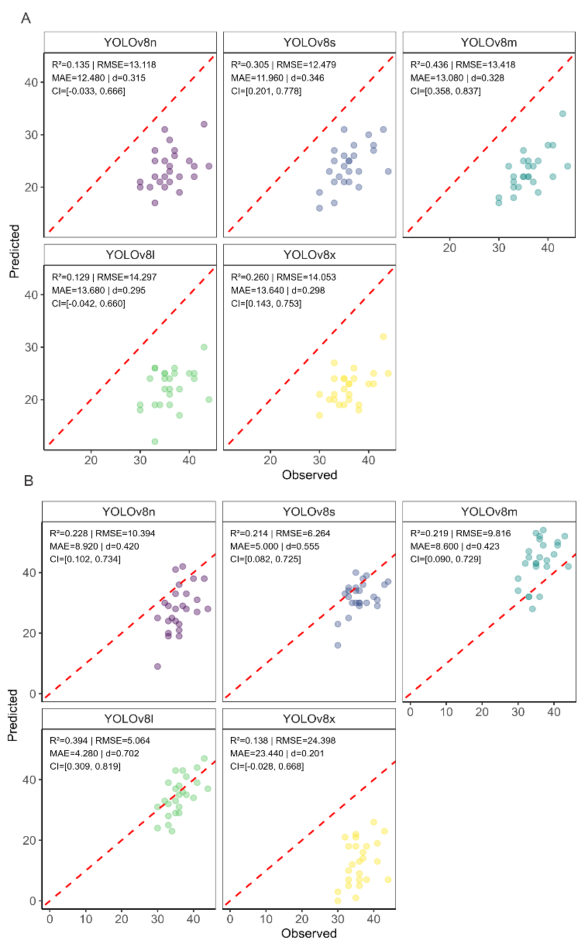

Figure 8. Scatter plots comparing the number of common bean plants observed in the field through manual counting and the number of plants predicted by the YOLOv8 models at the V2 phenological stage. Results are presented for flight heights of 20 and 40 m, represented by panels (A) and (B), respectively. Each panel shows the coefficient of determination (R^2), root mean square error (RMSE), mean absolute error (MAE), Willmott's agreement index (d), and confidence interval (CI).

The comparison between manual and automatic counting of common bean plants showed differences in model performance according to flight height and model architecture (Figure 8). At the flight height of 20 m (Figure 8A), most models showed a tendency to underestimate the number of plants, as most points were below the 1:1 line. Under this condition, the YOLOv8m model showed the highest coefficient of determination (R^2 = 0.436), followed by YOLOv8s (R^2 = 0.305) and YOLOv8x (R^2 = 0.260). However, RMSE and MAE values remained relatively high, indicating discrepancies between manual counting and model-estimated counting.

This underestimation may be associated with the difficulty of the models in detecting plants with different levels of early development and variation in leaf cover, even within the V2 stage. Leaf overlap, the proximity between plants, and the presence of similar plant structures may hinder the individual separation of plants, favoring the fusion of targets into a single point and leading to population underestimation (Furlanetto et al., 2025). In corn, Barboza, Santos, et al. (2026) also reported lower YOLOv9 performance at the V2 stage due to the small size of the plants and background interference, as well as reduced identification and counting at the V6 stage due to leaf overlap. Similarly, in applications using YOLOv8s to identify and count watermelons from UAV-acquired video frames, automatic identification also underestimated manual annotations because the algorithm prioritized temporal consistency and identity tracking over detection accuracy (Jiang et al., 2024).

For the flight height of 40 m (Figure 8B), the relationship between observed and predicted values showed better performance for some architectures, especially for the YOLOv8l model, which obtained the highest coefficient of determination (R^2 = 0.394), the lowest RMSE (5.064), and the lowest MAE (4.280). The YOLOv8s model also showed satisfactory performance, with RMSE and MAE values lower than those observed for most models. In contrast, the YOLOv8x model showed the highest estimation error, with an RMSE of 24.398 and an MAE of 23.440, indicating low prediction capacity under this condition.

The high error values observed in this study were greater than those reported by Oh et al. (2020), who obtained good performance in cotton plant counting using YOLOv3 under conditions in which plants were generally distinguishable from each other and density ranged from 0 to 14 plants per linear meter. However, those authors used images acquired at 10 m above ground level, a flight height that may be operationally limited for mapping large production areas due to both the greater demand for image acquisition in the field and the increased data processing time.

Overall, the results indicate that flight height influenced not only plant detection but also the accuracy of automatic counting. Images acquired at 20 m had a higher level of spatial detail; however, the greater presence of overlapping leaves, shadows, and nearby structures may have favored duplicate or inconsistent detections. In comparison, images acquired at 40 m had a lower level of spatial detail but, in some cases, provided a more homogeneous representation of the area, favoring automatic counting for specific models, such as YOLOv8l. These results indicate that the choice of flight height and model architecture should consider the balance between spatial resolution, visual complexity of the area, and the objective of the task.

Conclusions

This study demonstrates that RGB images acquired by UAVs, combined with YOLOv8 models, represent a promising approach for identifying and counting common bean plants during early growth stages. The V2 stage was challenging for automatic detection because the plants were small and close to the soil background. Even under these conditions, the models were able to detect common bean plants, although performance varied according to flight height and model architecture.

Flight height directly affected model performance. Images acquired at 20 m provided better overall detection results, especially with lightweight architectures such as YOLOv8n and YOLOv8s. At 40 m, detection performance decreased, but YOLOv8l showed the best performance among the evaluated architectures and also provided the best counting results.

Overall, the results highlight the potential of RGB images acquired by UAVs and YOLOv8 models to support the automated evaluation of the initial plant stand in common bean crops. This approach can reduce dependence on manual counting and improve the efficiency of early crop monitoring, allowing faster decision-making and timely actions, such as reseeding in areas with low plant establishment.

Acknowledgments

The authors gratefully acknowledge the Federal University of Lavras (UFLA), the Study Group in Precision Agriculture (GEPAD), the Coordination for the Improvement of Higher Education Personnel (CAPES), the National Council for Scientific and Technological Development (CNPq), the Foundation for Research Support of the State of Minas Gerais (FAPEMIG), and the Center for Development and Technology Transfer (CDTT/UFLA) for their support during the development of this study.

References

Alif, M. A. R., & Hussain, M. (2024). *YOLOv1 to YOLOv10: A comprehensive review of YOLO variants and their application in the agricultural domain*. http://arxiv.org/abs/2406.10139

Barboza, T. O. C., Fernandez, G. V., Inácio, F. D., Pinto, L. S., de Carvalho, A. A., Dos Reis, M. V., & Dos Santos, A. F. (2026). Detection and counting marigold flowers using drone images and YOLOv8 in complex environments. *Ornamental Horticulture*, *32*. https://doi.org/10.1590/2447-536X.v32.e323014

Barboza, T. O. C., Santos, A. F. dos, Bedwell, E. K., Vellidis, G., & Lacerda, L. N. (2026). Corn Plant Detection Using YOLOv9 Across Different Soil Background Colors, Growth Stages, and UAV Flight Heights. *Remote Sensing*, *18*(1). https://doi.org/10.3390/rs18010014

Biezus, A., Xavier, E., Brusamarello, A. P., Manteli, C., & Carvalho, A. F. G. (2017). Emergence and early development of bean seedlings at different sowing depths. Revista Brasileira de Ciências Agrárias, 12(4), 428–434. https://doi.org/10.5039/agraria.v12i4a5472

Chen, C., Zheng, Z., Xu, T., Guo, S., Feng, S., Yao, W., & Lan, Y. (2023). YOLO-based UAV technology: A review of the research and its applications. Drones, 7(3), 190. https://doi.org/10.3390/drones7030190

CONAB. (2026). Acompanhamento da safra brasileira de grãos: Safra 2025/26 – 6º levantamento. Companhia Nacional de Abastecimento.

Donato, F., Almeida, F. da S., Santana, M. J. de, & Xavier, A. G. (2022). Desempenho agronômico de cultivares de feijão comum em função da população de plantas. *Revista Inova Ciência & Tecnologia / Innovative Science & Technology Journal*, e0211122. https://doi.org/10.46921/rict2021-1122

FAO. (2023). *FAOSTAT: Crops and livestock products – Beans, dry*. Food and Agriculture Organization of the United Nations. https://www.fao.org/faostat/

Furlanetto, R. H., Boyd, N. S., & Buzanini, A. C. (2025). Multi-crop plant counting and geolocation using a YOLO-Powered GUI System. *Smart Agricultural Technology*, *11*. https://doi.org/10.1016/j.atech.2025.100994

Jiang, L., Jiang, H., Jing, X., Dang, H., Li, R., Chen, J., Majeed, Y., Sahni, R., & Fu, L. (2024). UAV-based field watermelon detection and counting using YOLOv8s with image panorama stitching and overlap partitioning. *Artificial Intelligence in Agriculture*, *13*, 117–127. https://doi.org/10.1016/j.aiia.2024.09.001

Kitano, B. T., Mendes, C. C. T., Geus, A. R., Oliveira, H. C., & Souza, J. R. (2019). Corn Plant Counting

Using Deep Learning and UAV Images. *IEEE Geoscience and Remote Sensing Letters*. https://doi.org/10.1109/LGRS.2019.2930549

Lu, C., Nnadozie, E., Camenzind, M. P., Hu, Y., & Yu, K. (2023). Maize plant detection using UAV-based RGB imaging and YOLOv5. *Frontiers in Plant Science*, *14*. https://doi.org/10.3389/fpls.2023.1274813

Oh, S., Chang, A., Ashapure, A., Jung, J., Dube, N., Maeda, M., Gonzalez, D., & Landivar, J. (2020). Plant counting of cotton from UAS imagery using deep learning-based object detection framework. *Remote Sensing*, *12*(18). https://doi.org/10.3390/RS12182981

Oliveira, G. M. de, & Wander, A. E. (2023). Mapeamento da cadeia produtiva do feijão-comum no Brasil Mapping the common beans production chain in Brazil. *Rev. Econom. Política Desenvolv*, *14*(32), 96–122. https://periodicos.ufal.br/repd/article/view/13558/11251

Quintela, E. D., & Barbosa, F. R. (2015). *Manual de Identificação de Insetos e Outros Invertebrados Pragas do Feijoeiro*. www.embrapa.br/fale-conosco/sac

Radoglou-Grammatikis, P., Sarigiannidis, P., Lagkas, T., & Moscholios, I. (2020). A compilation of UAV applications for precision agriculture. *Computer Networks*, *172*. https://doi.org/10.1016/j.comnet.2020.107148

Rana, A., & Vaidya, P. (2026). YOLO-based deep learning framework for real-time multi-class plant health monitoring in precision agriculture. *Scientific Reports*, *16*(1). https://doi.org/10.1038/s41598-025-29132-w

Sapkota, R., Meng, Z., Churuvija, M., Du, X., Ma, Z., & Karkee, M. (2026). Comprehensive performance evaluation of YOLOv12, YOLO11, YOLOv10, YOLOv9 and YOLOv8 on detecting and counting fruitlet in complex orchard environments. Agriculture Communications, 4(1), 100125. https://doi.org/10.1016/j.agrcom.2026.100125

Silva, S. C., & Heinemann, A. B. (2023). *Feijão: pré-produção: clima*. Embrapa – Empresa Brasileira de Pesquisa Agropecuária. https://www.embrapa.br/en/agencia-de-informacao-tecnologica/cultivos/feijao

Tsouros, D. C., Bibi, S., & Sarigiannidis, P. G. (2019). A review on UAV-based applications for precision agriculture. In *Information (Switzerland)* (Vol. 10, Number 11). MDPI AG. https://doi.org/10.3390/info10110349

Zhu, H., Lin, C., Liu, G., Wang, D., Qin, S., Li, A., Xu, J. L., & He, Y. (2024). Intelligent agriculture: Deep learning in UAV-based remote sensing imagery for crop diseases and pests detection. Frontiers in Plant Science, 15, 1435016. https://doi.org/10.3389/fpls.2024.1435016